Article ID: 1003－6326(2005)06－1237－05

R-phase transformation of aged Ti-Ni shape memory alloy①

GONG Chang-wei(宫长伟), WANG Yi-nong(王轶农),
YANG Da-zhi(杨大智), LIU Xiao-peng(刘晓鹏)
(Department of Materials Engineering, Dalian University of Technology,
Dalian 116024, China)

Abstract: Ti-50.6Ni(molar fraction, %) shape memory alloy solution treated at 850 ℃ for 1h followed by ageing treatment at 450 ℃ for 3 h was studied with differential scanning calorimetry(DSC), X-ray diffractometry(XRD) and transmission electron microscopy(TEM). DSC measurement reveals two separate transformation peaks. XRD and TEM demonstrate that a three-stage transformation occurs. The Ti_3Ni_4 precipitates are coherent with the *R*-phase. The crystal structure of *R*-phase was analyzed by two diffraction patterns method. The diffraction patterns of *R*-phase were obtained in detail from the same region.

Key words: Ti-Ni shape memory alloys; *R*-phase transformation; Ti_3Ni_4 precipitates
CLC number: TG 139.6 **Document code:** A

1 INTRODUCTION

The *B*2-*R* transformation in Ti-Ni shape memory alloy has attracted much attention in past decades since its small lattice distortion and temperature hysteresis. The small lattice distortion implies less damage to the microstructure and lower sensitivity to structure modifications, hence resulting in higher reversibility and stability. The small hysteresis implies high response rate and high reversibility. Owing to these unique characteristics, the *R*-phase transformation is of particular importance for many applications, such as actuators and sensors.

For the crystal structure of *R*-phase, it is still a controversial issue. Goo and Sinclair[1] studied the space group of the *R* phase using convergent beam electron diffraction. They reported the P31m space group, but the structure was not determined. Wu and Wayman[2] proposed a trigonal distortion of the cubic structure, which could appear by condensation of modes at the (1/3, 1/3, 1/3) reciprocal-lattice point. The phase transformation was described using an elongation of the cube along the body diagonal. The crystal structure of the *R* phase was analyzed by combined use of electron-diffraction and powder X-ray diffraction methods[3]. The *R*-phase belongs to the trigonal space group P3. But recently, Schryver and Potapov[4] proposed that the *R*-phase is trigonal space group P3 refined using the software package MSLS.

Because the pre-shaped treatment is usually used for various applications, the *B*2-*R* transformation occurs due to the aging treatment in Ni-rich Ti-Ni alloys (x(Ni) > 50.5%)[5－12]. Ti_3Ni_4 precipitates induce inhomogeneity of the matrix, both in terms of composition and internal stress fields, which favors the formation of *R*-phase prior to $B19'$[12－16]. For the mechanism of *B*2-*R* transformation, most work were based on the DSC measurements, and further experiments of microstructure observation are needed. In the present work, the *R* phase transformation was studied by DSC, XRD and TEM in detail in an aged Ti-50.6% Ni(molar fraction) alloy.

2 EXPERIMENTAL

Ti-50.6% Ni(molar fraction) alloy was solution treated at 850 ℃ for 1 h followed by quenching into water. Then it was aged at 450 ℃ for 3 h. To eliminate the effect of the oxide layer produced during heat treatment, the samples were chemically etched with an 1 mL HF+ 4 mL HNO_3+ 5 mL H_2O solution to remove the surface oxides, and mechanically polished using SiC paper in successive grades prior to DSC and XRD analysis.

The phase transformation characteristics of the aged samples were analyzed and determined with a Mettler DSC822^e instrument and a XRD-6000 X-ray diffractometer. A temperature range from － 60 to 150 ℃ was scanned at a rate of 10 ℃/min during cooling and heating. X-ray diffraction measurement was used to identify phase composition of specimens at room temperature. Specimens for the electron microscopy were prepared by jet

① **Foundation item:** Projects(50171015, 50471066) supported by the National Natural Science Foundation of China
Received date: 2005－03－11; **Accepted date:** 2005－05－28
Correspondence: GONG Chang-wei, PhD candidate; Tel: + 86-411-84708441; E-mail: cw_gong@sina.com

electronpolishing with a solution of 25% HNO_3 + 75% CH_3OH (volume fraction) at around − 30 ℃. For High-resolution image observation, the specimens high were finally argon ion polished to clear the surface contamination. TEM observations were carried out in a Philips Tecnai G^2 electron microscope operated at 200 kV, using FEI double-tilt specimen stage. The images were recorded using the GATAN CCD slow-scanning camera and then analyzed by the Digital Micrograph Software.

3 RESULTS AND DISCUSSION

3.1 Characteristics of *R*-phase transformation

The DSC result of the sample aged at 450 ℃ for 3 h is shown in Fig. 1. Two distinct peaks at cooling and two coterminous peaks upon heating are observed. To identify the transformation, XRD measurement is carried out at room temperature, as shown in Fig. 2. From the XRD measurement, we find that *B2*-phase and *R*-phase coexist at room temperature. This indicates a three-step phase transformation. The transformation temperatures in cooling are determined: R_s = 46 ℃, R_f = 28 ℃, M_s = − 3 ℃, M_f = − 43 ℃. The transformation temperatures in heating are determined: R'_s = 18 ℃, R'_f = 28 ℃, A_s = 34 ℃, A_f = 48 ℃. The *R*, *M*, *R*′ and *A* denote the transformation of $B2 \rightarrow R$, $R \rightarrow B19'$ (and $B2 \rightarrow B19'$), $B19' \rightarrow R$ and $R \rightarrow B2$ (and $B19' \rightarrow B2$), respectively. The subscript "s" denotes the temperature at which the phase transformation starts, and "f" denotes the temperature at which the phase transformation finishes.

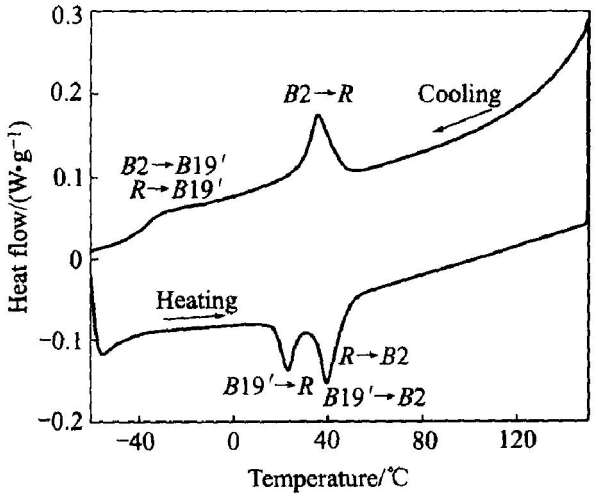

Fig. 1 DSC curves of Ti-50.6%Ni alloy aged at 450 ℃ for 3 h

A bright field image taken at room temperature, in which Ti_3Ni_4 precipitates can be clearly observed, is shown in Fig. 3. The corresponding diffraction pattern along $[111]_{B2}$ shown in Fig. 3 indicates that the region is in the *R*-phase. From

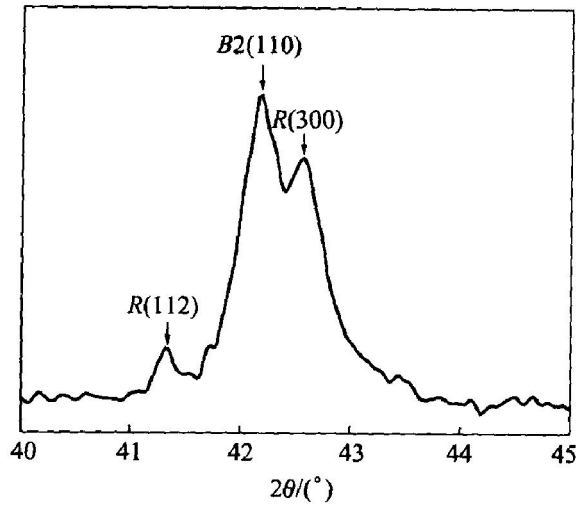

Fig. 2 XRD pattern of alloy at room temperature after ageing at 450 ℃ for 3 h

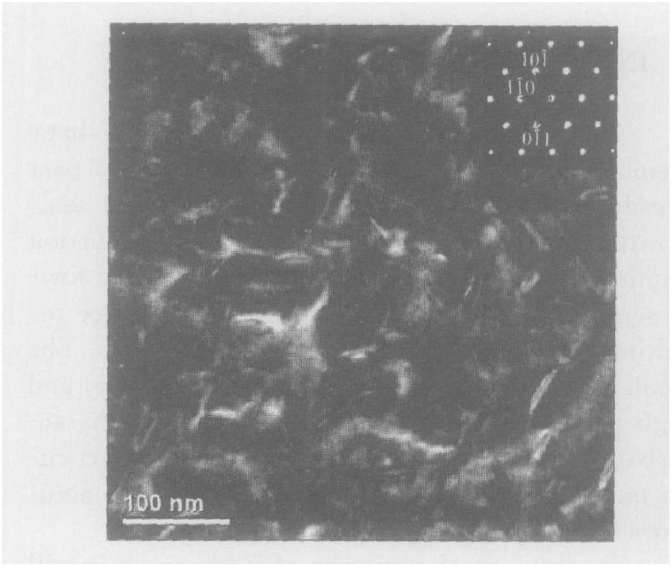

Fig. 3 Bright-field image of specimen at room temperature
(Inside is diffraction pattern of *R*-phase along $[111]_{B2}$)

Fig. 3, one can see that the Ti_3Ni_4 precipitates are nearly along $[\bar{1}10]$, $[10\bar{1}]$ and $[01\bar{1}]$ directions. The Ti_3Ni_4 precipitates can introduce internal tensile stress resulted from different density between the Ti_3Ni_4 and matrix (*B2*) and the misfit strain[5]. The stress state created by the presence of these precipitates decreases the barrier to *R*-phase transformation and the martensitic transformation that follows. The restriction of the Ti_3Ni_4 precipitates on the growth of the *R*-phase is indicated in Fig. 3, which confirms the suggestion that the high density of Ti_3Ni_4 precipitates in the matrix of the aged Ni-rich NiTi shape memory alloys is related to the smaller *R*-phase domain[2].

High resolution observations of the Ti_3Ni_4 precipitates and the *R*-phase are made in $[111]_{B2}$ zone, as shown in Fig. 4. In Fig. 4, the average Ti_3Ni_4 precipitate size is about 10 nm. The Ti_3Ni_4 precipitate is coherent with the *R* matrix. At the

same time, *B*2 phase can also be observed in some grain interior in this study. Fig. 5 shows high-resolution image of *B*2 matrix on (110) plane. The co-existence of *B*2 phase and *R*-phase in the aged Ti-Ni alloy agrees with the result of XRD measurement. In Ti-50.6% Ni alloy, the Ti_3Ni_4 preferentially precipitates near grain boundary, causing essentially precipitate-free zone at grain interior. This makes Ni content near grain boundary lower than that in the grain interior and the stress fields exit mainly near the boundary. The Ti_3Ni_4 precipitation induces the inhomogeneity of the matrix, both in composition and internal stress fields. Thus grain boundary portion undergoes two-stage *B*2-*R*-*B*19′ transformation while the grain interior undergoes a direct *B*2-*B*19′ transformation. This agrees with the low Ni supersaturation mode proposed in Ref. [15].

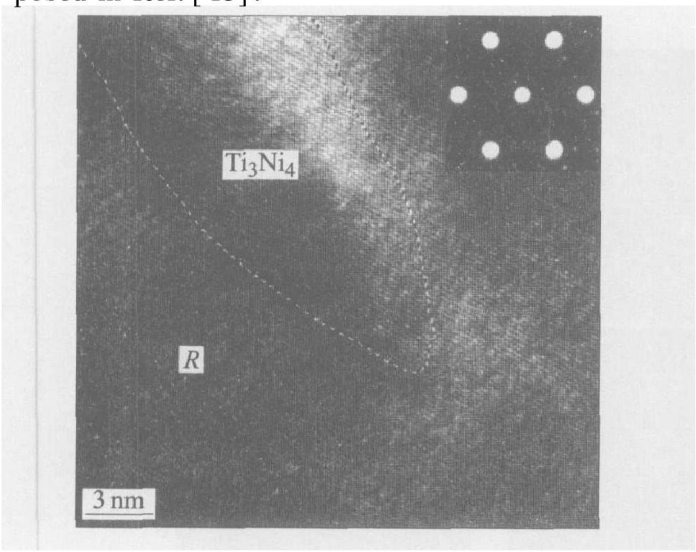

Fig. 4 HREM micrograph of Ti_3Ni_4 precipitates and *R*-phase along $[111]_{B2}$

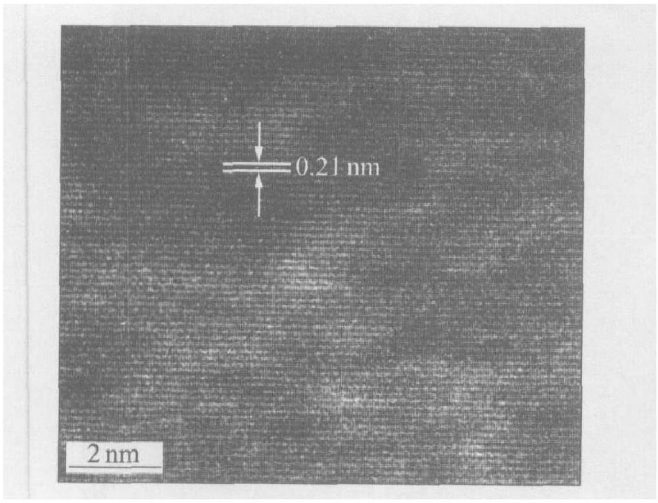

Fig. 5 HREM micrograph showing (110) plane of *B*2 matrix

3.2 Crystal structure of *R*-phase

In order to analyze the structure of *R*-phase, we take selected area diffraction patterns (SADPs) along $[111]_{B2}$ and $[\bar{1}2\bar{1}]_{B2}$ which are perpendicular to each other. The results are shown in Fig. 6. In Fig. 6, three vector $\boldsymbol{g}_1$, $\boldsymbol{g}_2$, $\boldsymbol{g}_3$ can be expressed as

$$\boldsymbol{g}_1 = \frac{1}{3}(\bar{1}10)_{B2} = \frac{1}{3}(\boldsymbol{a}^* - \boldsymbol{b}^*) \quad (1)$$

$$\boldsymbol{g}_2 = \frac{1}{3}(10\bar{1})_{B2} = \frac{1}{3}(\boldsymbol{a}^* - \boldsymbol{c}^*) \quad (2)$$

$$\boldsymbol{g}_3 = \frac{1}{6}(222)_{B2} = \frac{1}{3}(\boldsymbol{a}^* + \boldsymbol{b}^* + \boldsymbol{c}^*) \quad (3)$$

where $\boldsymbol{a}^*$, $\boldsymbol{b}^*$ and $\boldsymbol{c}^*$ are the basic vectors of *B*2 reciprocal space cell.

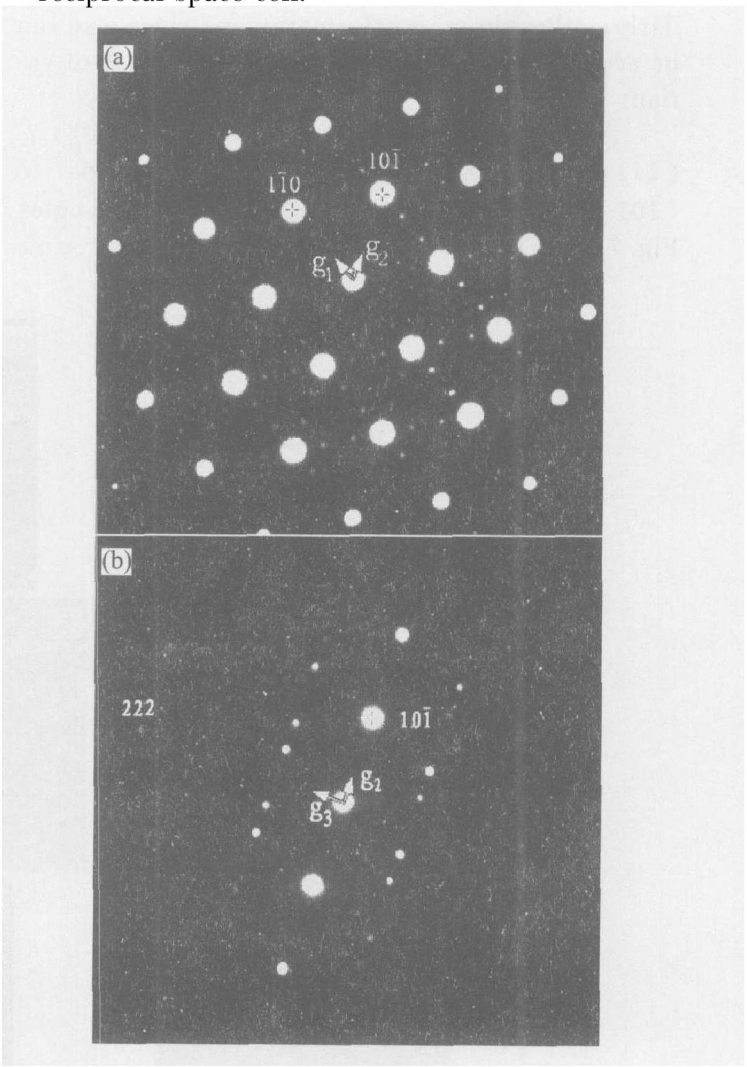

Fig. 6 Two SADPs along $[111]_{B2}$(a) and $[\bar{1}2\bar{1}]_{B2}$(b) perpendicular to each other from same region shown in Fig. 3

Thus the basic vectors of reciprocal space cell of super-structure, $\boldsymbol{a}_s^*$, $\boldsymbol{b}_s^*$, $\boldsymbol{c}_s^*$ can be determined:

$$\begin{bmatrix} \boldsymbol{a}_s^* \\ \boldsymbol{b}_s^* \\ \boldsymbol{c}_s^* \end{bmatrix} = \frac{1}{3}\begin{bmatrix} 1 & \bar{1} & 0 \\ 1 & 0 & \bar{1} \\ 1 & 1 & 1 \end{bmatrix}\begin{bmatrix} \boldsymbol{a}^* \\ \boldsymbol{b}^* \\ \boldsymbol{c}^* \end{bmatrix} \quad (4)$$

According to the relationship between the real space and reciprocal space, then

$$\begin{bmatrix} \boldsymbol{a}_s \\ \boldsymbol{b}_s \\ \boldsymbol{c}_s \end{bmatrix} = \begin{bmatrix} 1 & \bar{2} & \bar{1} \\ 1 & 1 & \bar{2} \\ 1 & 1 & 1 \end{bmatrix}\begin{bmatrix} \boldsymbol{a} \\ \boldsymbol{b} \\ \boldsymbol{c} \end{bmatrix} \quad (5)$$

where $\boldsymbol{a}_s$, $\boldsymbol{b}_s$, $\boldsymbol{c}_s$ are the basic vectors of real space cell of super-structure; $\boldsymbol{a}$, $\boldsymbol{b}$, $\boldsymbol{c}$ are the basic vectors of $B2$ real space cell. Thus the transformation matrix can be expressed as

$$\boldsymbol{T}=\begin{vmatrix} 1 & \bar{2} & \frac{1}{2} \\ 1 & 1 & \frac{1}{2} \\ 1 & 1 & 1 \end{vmatrix} \tag{6}$$

Because the $B2$ matrix is of cubic structure, the R-phase super-structure is of hexagonal structure. The transformation matrix in Eqn. (6) is consistent with the result of variant A[1, 5, 12]. Similarly, other three transformation matrixes also can be acquired, which correspond to the results of variant B, C, and D.

According to Eqn. (6), $(010)_{B2}$-$(110)_{B2}$-$(\bar{1}11)_{B2}$ stereographic triangle corresponds to $(\bar{1}01)_R$-$(012)_R$-$(001)_R$ stereographic triangle. Fig. 7 shows the results of SADPs from the same region in bright field image shown in Fig. 3. In Fig. 7, there are 12 Laue index zones along or within the $(\bar{1}01)_R$-$(012)_R$-$(001)_R$ stereographic triangle. They are consistent with the results in Ref. [2]. From Fig. 7, one can observe sharp high-intensity $\frac{1}{3}$-reflections with no surrounding streaking or diffuse-scattering. When we analyze the result of electron diffractions, we find that the extra-spot situates at the $\frac{1}{3}\langle 111\rangle_{B2}$ and $\langle 110\rangle_{B2}$ positions. Because of the difference between P3 and P$\bar{3}$, from the electron diffractions we can't determine the space group of R-phase. Thus we compare them from the first calculation. The result indicates that the P3 gives the lower ground energy and is more stable than P$\bar{3}$. Thus the R-phase belongs to the trigonal space group P3.

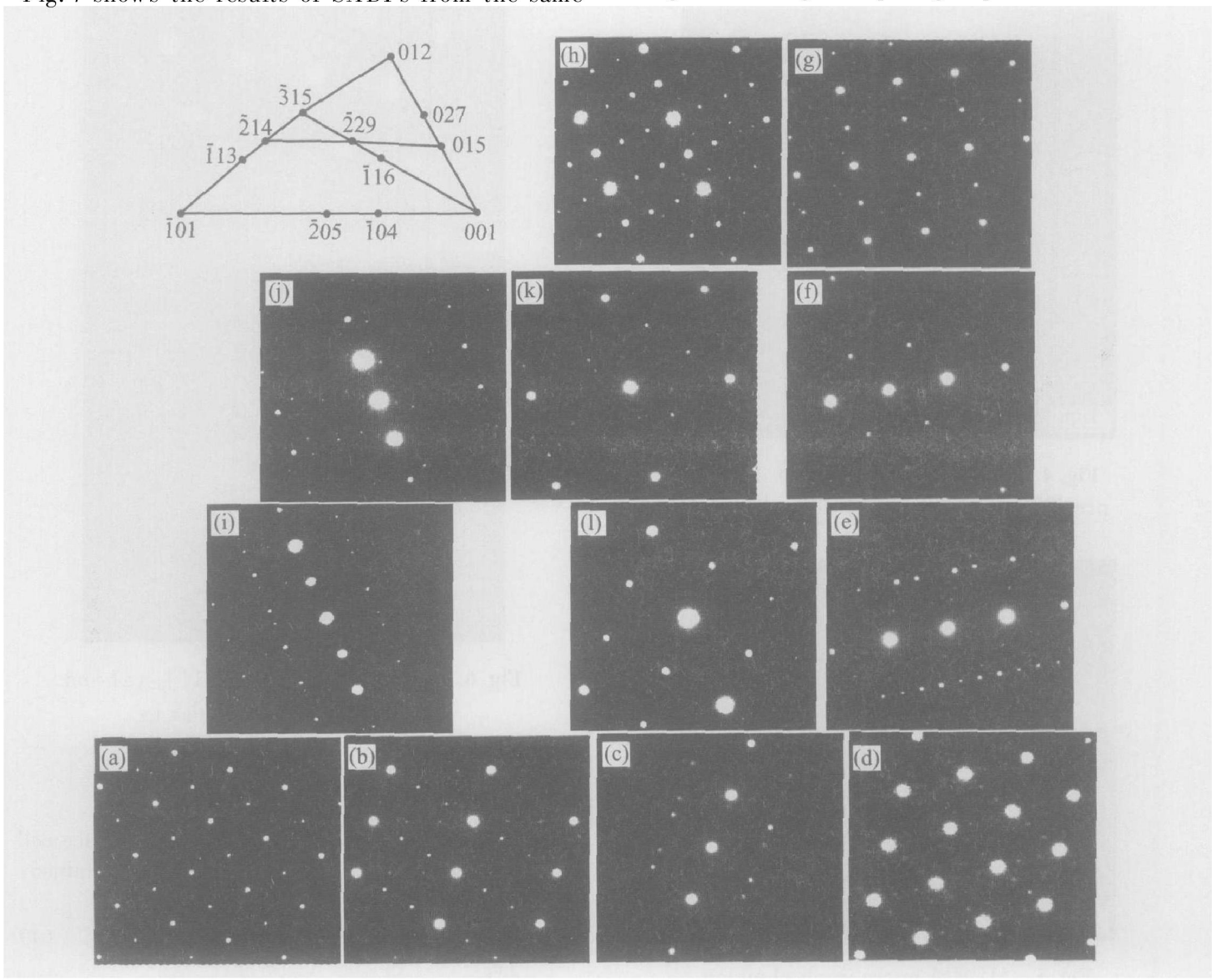

Fig. 7 SADPs of Fig. 3 main Laue index zones along or inside $[\bar{1}01]_R$-$[012]_R$-$[001]_R$ triangle
(a) $\rightarrow[\bar{1}01]$; (b) $\rightarrow[\bar{2}05]$; (c) $\rightarrow[\bar{1}04]$; (d) $\rightarrow[\bar{0}01]$; (e) $\rightarrow[\bar{0}15]$; (f) $\rightarrow[\bar{0}27]$; (g) $\rightarrow[012]$; (h) $\rightarrow[\bar{1}13]$; (i) $\rightarrow[\bar{2}14]$; (j) $\rightarrow[\bar{3}15]$; (k) $\rightarrow[\bar{2}29]$; (l) $\rightarrow[\bar{1}16]$

4 CONCLUSIONS

1) It is found that a three-stage transformation occurs in the aged Ti-Ni shape memory alloy. It is contributed to Ti_3Ni_4 precipitation-induced inhomogeneity of the matrix, both in composition and internal stress fields. The Ti_3Ni_4 precipitates are coherent with the *R*-phase.

2) The $B2 \rightarrow R$ transformation matrix was obtained. The *R*-phase belongs to the trigonal space group P3.

REFERENCES

[1] Goo E, Sinclair R. The *B*2 to *R* transformation in $Ti_{50}Ni_{47}Fe_3$ and $Ti_{49.5}Ni_{50.5}$ alloys[J]. Acta Metall, 1985, 33: 1717-1723.

[2] Wu S K, Wayman C M. On the reciprocal lattice of the "premartensitic" *R*-phase in TiNi shape memory alloys[J]. Acta Metal, 1989, 37: 2805-2813.

[3] Hara T, Ohba T, Okunishi E, et al. Structure study of *R*-phase in Ti-50.23at.% and Ti-47.75at.% Fe alloys[J]. Materials Transactions JIM, 1997, 38: 11-17.

[4] Schryver D, Potapov P. Electron diffraction refinement of the TiNi(Fe) *R*-phase structure[J]. J Phys Ⅳ, 2003, 112: 751-754.

[5] Li D Y, Wu X F, Ko T. The effect of stress on soft modes for phase transformations in a Ti-Ni alloy (Ⅱ)—Effects of ageing and thermal cycling on the phase transformations[J]. Phil Mag A, 1991, 63: 603-616.

[6] Xie C Y, Zhao L C, Lei TC. Effect of precipitates on the electrical resistivity—temperature curves in an aged Ti-50.8at% Ni shape memory alloy[J]. Scripta Metallugica, 1989, 24: 2132-2136.

[7] Nishida M, Wayman C M. Electron microscopy studies of the premartensitic transformations in an aged Ti-51at% Ni shape memory alloy[J]. Metallography, 1988, 21: 255-273.

[8] Cai W, Murakami Y, Otsuka K. Study of *R*-phase transformation in a Ti-50.7at% Ni alloy by in-situ transmission electron microscopy observations[J]. Mater Sci Eng A, 1999, 273-275: 186-189.

[9] Miyazaki S, Wayman C M. The *R*-phase transition and associated shape memory mechanism in Ti-Ni single crystals[J]. Acta Metal, 1988, 36: 181-192.

[10] Stróz D. TEM studies of the *R*-phase transformation in a NiTi shape memory alloy after thermo-mechanical treatment[J]. Materials Chemistry and Physics, 2003, 81: 460-462.

[11] Tan L, Crone W C. In situ TEM observation of two-step martensitic transformation in aged NiTi shape memory alloy[J]. Scripta Materialia, 2004, 50: 819-823.

[12] Kim J I, Liu Yinong, Miyazaki S. Ageing-induced two-stage *R*-phase transformation in Ti-50.9at.% Ni[J]. Acta Materialia, 2004, 52: 487-499.

[13] Ren X, Miura N, Taniwaki K, et al. Understanding the martensitic transformation in TiNi-based alloys by elastic constants measurement[J]. Mater Sci Eng A, 1999, A273-275: 190-194.

[14] Khalil J, Ren X, Eggeler G. The mechanism of multistage martensitic transformations in aged Ni-rich Ni-Ti shape memory alloys[J]. Acta Materialia, 2002, 50: 793-803.

[15] Fan G, Chen W, Yang S, et al. Origin of abnormal multi-stage martensitic transformation behavior in aged Ni-rich Ti-Ni shape memory alloys[J]. Acta Materialia, 2004, 52: 4351-4362.

[16] Jafar K A, Antonin D, Gunther E. Ni_4Ti_3-precipitation during aging of NiTi shape memory alloys and its influence on martensitic phase transformations[J]. 2002, 50: 4255-4274.

(Edited by YANG Bing)